View Article Online
View Journal

Green Chemistry

Cutting-edge research for a greener sustainable future

Accepted Manuscript

This article can be cited before page numbers have been issued, to do this please use: K. Ouyang, W. Munib, Q. H. Lê, L. Leskinen, Y. Wu, N. Chenna, I. Schlapp-Hackl and J. Dou, *Green Chem.*, 2026, DOI: 10.1039/D6GC01257D.

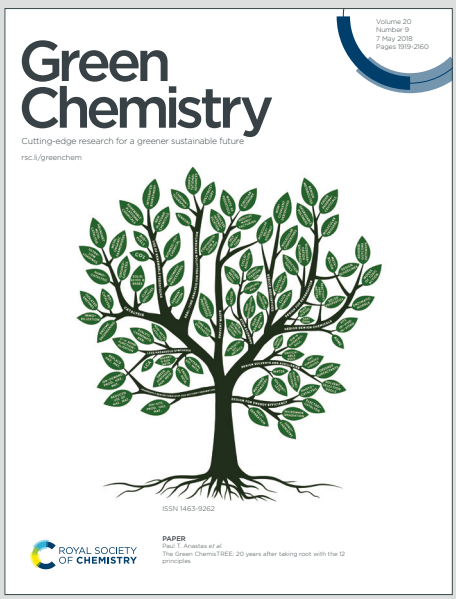

View Article Online
DOI: 10.1039/D6GC01257D

1. The industrial valorization of bagasse is currently hampered by the inefficiency in bleaching chemical use and the limitations of alkali recovery out of silica-rich spent liquors. Our study establishes an integrated biorefinery strategy combining acid hydrolysis pretreatment (A-stage) for reducing usage of bleaching chemicals along with membrane-based fractionation of spent liquor.
2. In the fiber line, incorporating an A-stage prior to ECF bleaching selectively removed half of HexA and reduced ClO2 consumption by 25%. Possible migration of silica from its free form SiO2 at bagasse to form of CaSiO3 at the pulp is discovered. Ultrafiltration utilizing a 0.5 kDa-sized membrane retained HMW lignin-xylan complex in the retentate while allowing the permeation of 72%-recoverable hydroxy acids and alkali.
3. Future research shall tailor acid charge and temperature into a balance between chemical savings and pulp quality. Fine-tuning is needed to maintain separation stability of hydroxy acids and alkali recovery from permeate.

View Article Online
DOI: 10.1039/D6GC01257D

Towards sustainable pulping of bagasse: silica migration, hexenuronic acid removal and ultrafiltration-based spent liquor utilization

Kun Ouyang[a]; Wajeeha Munib[a]; Quang Huy Lê[a]; Lauri Leskinen[a]; Yue Wu[a]; Naveen Chenna[b]; Inge Schlapp-Hackl[a]; Jinze Dou*[a]

[a]Department of Bioproducts and Biosystems, Aalto University, Vuorimiehentie 1, Espoo, Finland
[b]Andritz Oy, Tammasaarenkatu 1, Helsinki, Finland

*E-mail: jinze.dou@aalto.fi; Tel: +358 504088797

Abstract

Transforming the utilization of agricultural residues from single-purpose papermaking into high-value biorefinery strategies can unlock their full potential. The industrial valorization of bagasse is currently hampered by the inefficiency in bleaching chemical use and the limitations of alkali recovery out of silica-rich spent liquors. To address these challenges, this study establishes an integrated biorefinery strategy combining acid hydrolysis stage (A-stage) for reducing usage of bleaching chemicals along with membrane-based fractionation of spent liquor. In the fiberline, incorporating an A-stage prior to elemental chlorine-free (ECF) bleaching selectively removed half of hexenuronic acid (HexA). This targeted elimination reduced chlorine dioxide (ClO_2) consumption by 25% despite an expected compromise in losing viscosity of bleached pulp fiber. Possible hypothetical migration (fate) of silica from its free amorphous silica form (SiO_2) at bagasse to primary form of calcium silicate ($CaSiO_3$) at the pulp fiber is discovered. Ultrafiltration utilizing a 0.5 kDa-sized membrane retained high-molecular-weight lignin-xylan complex in the retentate while allowing the permeation of 72%-recoverable hydroxy acids (enriched with 2-hydroxybutanoic acid and glucoisosaccharinic acid) and alkali from permeate, opening up the promise of applying a tailored ultrafiltration separation in addressing limitations in alkali recovery for spent liquor fractionation for bagasse mill.

Keywords: Alkali recovery; Bagasse; Calcium silicate; Hexenuronic acid; Hydroxy acids; Silica migration; Ultrafiltration

View Article Online
DOI: 10.1039/D6GC01257D

Introduction

Nowadays, non-wood raw materials, especially agricultural residues, are seen as potential alternatives to wood-based feedstock in the pulp and paper industry, contributing to reduce dependence on forest resources. Among these, bagasse, a well-known agricultural industrial residue, is considered a highly promising biorefinery feedstock due to its rapid renewability and widespread availability in regions such as Brazil, India, and China.[1] However, the full valorization of bagasse still presents challenges. Hexenuronic acid (HexA) groups present in xylan consume additional bleaching chemicals, although HexA content in bagasse kraft pulp (16.5 μmol/g) is significantly lower than that in unbleached kraft pulp of softwood (21.8 μmol/g) and eucalyptus (50.45 μmol/g).[2-4] The conventional Tomlinson recovery boiler is generally not economically or volumetrically tailored for bagasse pulp mills due to the chemical profile differences of spent liquor out of wood and non-wood.[5]

Hexenuronic acid (HexA) is a critical side-product formed during the alkaline pulping of xylan-rich biomass. Under high-temperature alkaline conditions, the 4-*O*-methyl-D-glucuronic acid side groups on xylan undergo *β*-elimination, releasing methanol and generating the unsaturated HexA structure.[6,7] Its electron-rich C=C contributes to kappa number and rapidly consumes electrophilic bleaching chemicals. To mitigate this, the acid hydrolysis stage (A-stage) is developed for treating pulp at pH 3.0–3.5 and 85–95°C for 1–2 hours,[7] through which could selectively cleave over 80–90% of HexA groups with minimal hemicelluloses degradation. Selective acid hydrolysis can remove HexA (20-60 μmol/g pulp) along with 2-7 units reduction of kappa, 30-40% of bleaching chemical can be saved for example in ECF bleaching of birch kraft pulp.[7] D-hot pretreatment (D-hot, 85°C) removed approximately 19% more HexA (**Table 1**) and reduced the generation of AOX by about 35% compared to conventional D_0 (60°C) stage.[2] The key differences between A/Do and D-hot is when HexA are removed relative to chlorine dioxide treatment. Hydrolysis of HexA -origin hemicelluloses can also be achieved biologically by xylanase (**Table 1**).[8]

Table 1 Comparative studies of bleaching pretreatment (regular font) and spent liquor fractionation (*italic*) based on the conventional strategy and our strategy.

Strategy	Methodology	Mechanism	Pulp (or NaOH%) / biomass	Main findings	Ref
Conventional (bleaching)	D-hot (T 95 °C, pH 3.2, t 1h)	HexA hydrolysis happens after ClO2 oxidation	Unbleached pulp/ bagasse	19% more HexA removal; brightness increase; kappa reduced 11% with D-hot	2
	xylanase (0-25 IU/g) (T 65 °C, pH 9, t 2h)	hydrolysis of HexA -origin hemicelluloses by hemicellulases	Unbleached pulp/ bagasse	reduction of 21.4–26.6% AOX and 12.5–22% ClO_2 with xylanase	8
Conventional (spent liquor)	*weak cation exchange resin in Na+ form*	*reversible electrostatic interaction to separate charged ions*	*22 %NaOH; T165°C/ birch*	*50% recovery of hydroxy acids (HAs) along with 95% lignin*	*12*
	5,10 and 15 kDa cut-offs	*membrane separation on basis of size*	*7.5% NaOH; T 90°C/ grass*	*5/15 kDa-sized permeate comprise high fractions of low molecular weight lignin*	*13*
	5,15 and 50 kDa cut-offs	*membrane separation on basis of size*	*23% NaOH; T 152 °C/ Eucalyptus globulus*	*retentate of 50 kDa obtained more lignin; 5 kDa permeate contain phenolic monomers*	*14*
Our strategy	A-stage (pH 3.5, T 95 °C, 2h); *0.5 kDa cut-off*	HexA hydrolysis increases along with decreasing pH; *membrane separation on basis of size*	Unbleached pulp; *15 % NaOH; T 165°C/* bagasse	25% savings of ClO_2; *73% recovery HAs from permeate and lignin-xylan complex from retentate; silica migration is observed*	This study

View Article Online
DOI: 10.1039/D6GC01257D

Another shift is also required regarding the utilization of spent liquor from non-wood pulp mills. Traditionally, this stream is concentrated (dry solids content increases from 14-16% to 75-85%) at evaporation plant and combusted for energy at recovery boiler and alkali recovery through the lime kiln and causticizing plant (**Fig. 1b**). However, this approach represents an undervaluation of organic resources, particularly for bagasse liquors with much lower calorific values. Moreover, soda cooking has been a significant method for pulping bagasse. During alkaline cooking, approximately 40–50% of the initial carbohydrates degrade via the "peeling reaction" into low-molecular-weight HAs, including lactic acid, glycolic acid, and 2-hydroxybutanoic acid.[9,10] These C1–C6 organic acids can be catalytically upgraded to carboxylic acid products.[11] 50% of HAs and over 95% of lignin can be recovered from soda and kraft black liquors through an ion exchange chromatographic method (**Table 1**).[12] To address the challenge of separating these small molecules from macromolecular lignin, membrane ultrafiltration (UF) has emerged as a promising strategy. Utilizing UF membranes with specific molecular weight cut-offs (MWCO, e.g., 1–5 kDa) can effectively fractionate the industrial kraft black liquor, from where the retentate comprises high-purity lignin while the permeate recovers a filtrate rich in HAs and residual alkali (**Table 1**).[13,14]

To address these technical challenges, this study proposes an integrated biorefinery strategy combining targeted reduced usage of bleaching chemicals along with membrane-based recovery of process chemicals for fiberline of bagasse. Specifically, we investigated the introduction of an acid hydrolysis stage (A-stage) prior to elemental chlorine-free (ECF) bleaching, aimed at selectively removing HexA to minimize use of bleaching chemicals. Moreover, ultrafiltration paves the promise as a pretreatment step for recovery of alkali, lignin-xylan complex along with HAs prior their incineration at power boiler for energy supply. However, ultrafiltration step alone is not positioned as a stand-alone technological alternative to alkali recovery furnace infrastructure. The long-term vision (or concept) is to replace the existing recovery boiler (and evaporation unit) with a much smaller and financially more affordable alternative solutions like simplified membrane and power boiler unit for closing the alkali recovery cycle and meeting energy demand of bagasse mill typically having pulp production 100-500 air-dried tons per day (ADt/d).

Materials and methods

Raw materials and chemicals

The bagasse feedstock was procured from Guangxi Yongxin Huatang Group (China). Prior to shipment to Finland, the biomass underwent an overnight air-drying process at 50 °C to stabilize moisture content. For the spent liquor fractionation, flat sheet polyethersulfone (PES) membranes (NADIR® NP030) with a MWCO of 0.5 kDa were acquired from MANN+HUMMEL (Germany).

All chemicals were of analytical grade and used as received without further purification. Regarding chemical reagents, the chlorine dioxide (ClO_2) was supplied by Kemira Oyj (Finland). General reagents for pulping and bleaching, including sulfuric acid (H_2SO_4, 95–97 w/w%), sodium hydroxide (NaOH, 98.5–100%), and hydrogen peroxide (H_2O_2, 30%) were purchased from VWR International (Finland). Hydrochloric acid (HCl , 37 w/w%) and magnesium sulfate ($MgSO_4$, 99.5%) were obtained from Merck KGaA (Germany). For analytical characterization, the silylation agents O-Bis(trimethylsilyl)trifluoroacetamide (BSTFA) containing 1% trimethylchlorosilane (TMCS) along with deuterated solvents for NMR (dimethyl sulfoxide-d_6, 99.9 atom % D; pyridine-d_5) were sourced from VWR (Finland). Additional analytical standards and reagents included: tetracosane and pyridine (Merck) for GC-MS analysis; sodium formate and 2-furoic acid (MedChemExpress, Sweden) for HexA determination and nitric acid for ICP-OES (Sigma-Aldrich). Reagents for iodometric titration, including sodium thiosulfate ($Na_2S_2O_3$), potassium iodide (KI), ammonium molybdate (catalyst for H_2O_2 determination), and starch were obtained from Sigma-Aldrich.

Experimental procedures

View Article Online
DOI: 10.1039/D6GC01257D

Pretreatment and pulping. The raw bagasse was first screened using an allgaier device (Allgaier Process Technology GmbH, Germany) to remove non-fibrous parenchyma cells, fines and dust (< 3 mm). This screened fibrous bagasse (**B**, 40 w/w% raw bagasse, **Table S1**) was used as the feedstock for all subsequent experiments. For consistency, all chemical dosages, pulp yields, and quantitative analyses reported in this study are calculated based on the oven-dry weight of fibrous bagasse (B). To mitigate silica scaling and enhance delignification, a two-step pretreatment was applied at **Fig. 1**. First, water washing was conducted using a stainless-steel reactor at 55–60 °C for 30 min (liquid:solid, L:S, 20:1) to remove water-soluble extractives. Subsequently, an alkali wash was performed using 1 M NaOH (L:S, 10:1) at 60–62 °C for 60 min in a pressurized air-bath reactor (Haato-tuote, Model 16140-538) (Haato Oy, Finland) ideally for leaching silica and waxes. Soda cooking was carried out in the same reactor using an active alkali charge of 15% (as NaOH). The cooking profile consisted of heating to 165 °C and holding for 60 min (H-factor, 611), the alkali wash and soda cooking were both performed under N_2 atmosphere. The cooked pulp was separated from the soda spent liquor by filtration using a nylon pulping bag (particle size of 50 µm). The pulp was washed and screened (0.35 mm slot) using Mänttä flat screener (G.A. Serlachius, Finland), while the spent liquor was collected and stored for analytics and further ultrafiltration treatments.

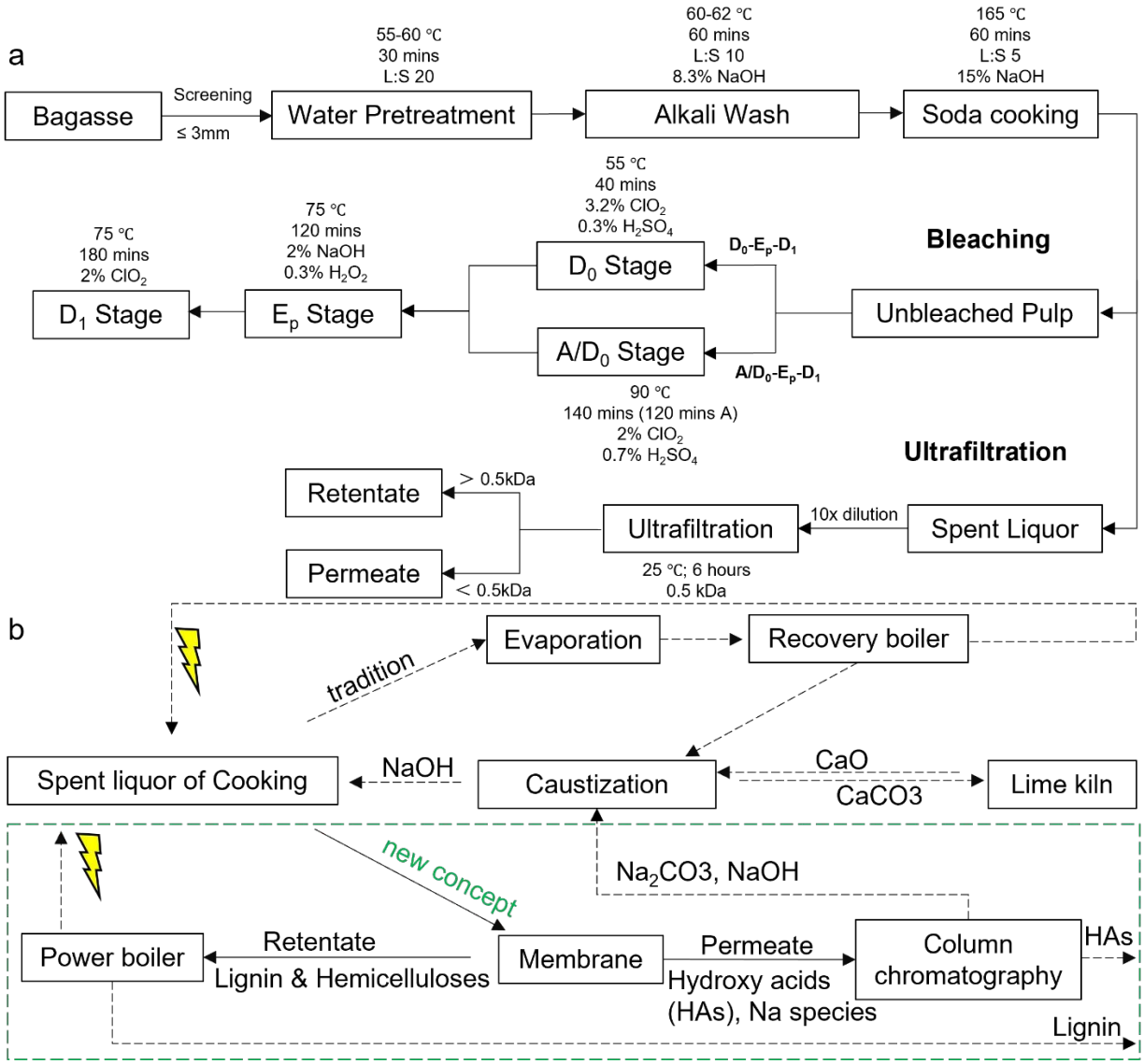

Fig. 1 Methodology and long-term vision. a Experimental flow of the bleaching and ultrafiltration after soda-cooking of bagasse; **b** Outlook of our concept is highlighted in green dashed line; dashed

View Article Online
DOI: 10.1039/D6GC01257D

arrow lines are used to indicate theoretical frameworks however out of scope of this present study. The applied analytics are summarized at **Table S1.**

Soxhlet extraction. The fibrous bagasse (B) was subjected to a successive Soxhlet extraction on the same batch to remove lipophilic extractives and waxes. Approximately 10 g of the air-dried biomass was successively extracted with dichloromethane (DCM) and acetone in a Soxhlet apparatus. The extracted solid residue was then air-dried to remove residual solvent before the complete drying using the freeze dryer and finally stored in a desiccator for subsequent experiments.

Bleaching sequences. Two ECF sequences include a standard D_0-E_p-D_1 sequence and a modified A/D_0-E_p-D_1 sequence incorporating an A-stage. The conditions and chemical charge are listed (**Fig. 1**). Bleaching experiments were performed in sealed 1 L-sized borosilicate glass vessels (Duran) immersed in a thermostat water bath (Kottermann GWB, Germany). Two ECF sequences were evaluated to determine the efficacy of HexA removal and delignification. Following each stage, the pulp was thoroughly washed with excessive water in plastic bucket by manual mixing, followed by centrifugation to collect the bleaching filtrates. The concentrations of ClO_2 and H_2O_2 were titrated following TAPPI T 611 cm-07.

Membrane fractionation of spent liquor. Spent liquor fractionation was executed using a 6-layer filter discs module (LabStak M20-0.72, Alfa Laval, Sweden) fitted with a stack of 12 polyethersulfone (PES) flat-sheet 0.5 kDa-sized membranes having membrane area of 0.018 m^2 /membrane (NP030P, MANN+HUMMEL, Germany). To ensure seal integrity and prevent leakage during the operation, the membrane stack was hydraulically compressed to a closing pressure of 375 bar for holding the filter plates together. Pressure for inlet and outlet of the membrane stack are 12 bars and 7.5 bars, respectively. The pressure difference must be kept in roughly 5 bars to have back pressure for the membranes, otherwise the membranes would burst through the holes of the disks. The inlet pressure is set with rotational speed of the pump motor, and the pressure difference can be adjusted with the tap underneath the outlet pressure gauge assembly. The entire filtration process was conducted at an ambient temperature to minimize thermal degradation of the analytes. The spent liquor initially fed into the ultrafiltration system is referred as “feed”. The feed is divided into two distinct streams during the membrane separation, the “retentate” contains macromolecules that cannot pass through the membrane pores however the “permeate” is the filtrate portion contain small molecules that can pass through the membrane. Once stabilized, one complete cycle (equal to 6 hours) of aliquots of both the permeate and retentate streams were sampled for characterization, and the re-captured retentate from the preceding cycle served as the feed for the subsequent stage of ultrafiltration. Two additional cycles of permeate were collected for calculating flux decline curves over the initial measured permeate flux out of first cycle of collection.

Characterizations

Pulp properties. The kappa, viscosity, and ISO brightness were determined according to SCAN-C 1:00, SCAN-CM 15:99, and SCAN-P 3:93, respectively. Prior to morphological analysis, pulp samples were dispersed in deionized water to achieve a highly diluted suspension of 0.01% (w/w). Paper sheets (optical properties) were prepared following SCAN-CM 11:95. Tensile measurements were done in conditions according to ISO 187:2022 under constant temperature (23 °C) and humidity control (50%). Thickness was determined according to ISO 534. Tensile strength tests were done according to ISO 1924-3 by Lorentzen and Wettre’s horizontal tensile tester MTS 400 (MTS system Norden, Sweden) with load cells of 200N.

All preparatory and analytical steps were conducted under controlled ambient conditions. The surface topography and structural integrity of the bagasse fibers were characterized using a Scanning Electron Microscope (FE-SEM, Zeiss Sigma VP, Germany). The samples were sputter-coated with platinum/palladium (pt/pd). Imaging was performed with the accelerating voltage between 5 and 10

View Article Online
DOI: 10.1039/D6GC01257D

kV. Tescan Mira 3 Sem with Oxford Instruments Xplore30 EDS is employed for the SEM-EDX analysis under acceleration voltage of 5 kV and beam intensity of 13 (beam current 880 pA). Beam measurement was conducted with the aluminum before the analysis; the quantification was done with factory-standard that is supplied by Oxford Instruments. B-P1-P2-C paper sheet with a 20 nm thick carbon layer is used for the analysis. X-ray diffraction (XRD) patterns of pulp were recorded using a Bruker D8 Advance powder diffractometer equipped with a Cu Kα radiation source (λ = 0.1542 nm), operated at 40 kV and 40 mA. Data were collected at 25 °C over a 2θ range of 10–60°, with a step size of 0.01° and a counting time of 1 s per step. X-ray photoelectron spectroscopy (XPS) were performed with a Kratos AXIS Ultra DLD X-ray photoelectron spectrometer using a monochromated AlKα X-ray source (1486.7 eV) run at 100 W. A pass energy of 80 eV and a step size of 1.0 eV were used for the survey spectra, while a pass energy of 20 eV and a step size of 0.1 eV were used for the high-resolution spectra. Photoelectrons were collected at a 90° take-off angle under ultra-high vacuum, with a base pressure typically below 1 x 10-9 TorrBoth survey and high-resolution spectra were collected from three different spots on the sample surface to check for homogeneity and surface charge effects. High-resolution have been charge-corrected with respect to the position of C-O bonding in cellulose at 286.5 eV, corresponding to a C-C binding energy of 284.8 eV.

HexA content. Hexenuronic acid content was quantified by UV spectrophotometry following a selective acid hydrolysis protocol.[15] Approximately 2.5 g of oven-dried pulp was suspended in 150 mL of 0.01 M sodium formate buffer (pH 3.5) within a sealed pressure-resistant glass vessel (Duran), nitrogen gas was purged immediately before closing the cap for hydrolysis. Hydrolysis was conducted in an autoclave (Systec DE 23, Germany) at a controlled temperature of 110 °C for 60 minutes. Ice bath was used for quenching the reaction. Under these acidic conditions, HexA groups are selectively cleaved from the xylan backbone and degraded primarily into 2-furoic acid and 5-carboxy-2-furaldehyde, the concentration of which was determined by measuring its absorbance at 245 nm. Upon completion, the reaction mixture was cooled to ambient temperature, and the liquid phase was separated from the fiber matrix by vacuum filtration through a Büchner funnel. The filtrate, combined with subsequent washings, was volumetrically adjusted to 1 L using deionized water. Spectral acquisition was performed using a Shimadzu UV-2550 spectrophotometer (Japan) across 200–500 nm. The specific absorbance was recorded at 245 nm (A_{245}), with a background correction applied at 480 nm (A_{480}) to eliminate the interference from non-specific chromophores. For samples exceeding an absorbance of 1.5, appropriate dilution was performed to maintain linearity. The final HexA content (c, in umol/g) was calculated according to Equation (1), utilizing an extinction coefficient factor derived from 2-furoic acid's calibration.

$$c = \frac{A_{245} - A_{480}}{8.7 \times m} \quad (1)$$

where m represents the oven-dried mass of the pulp sample in grams.

Chemical composition. Carbohydrate composition was analyzed by high-performance anion-exchange chromatography with pulsed amperometric detection (HPAEC-PAD, Dionex ICS 5000) following two-step acid hydrolysis (NREL/TP-510-42618).[16] Inorganic elements were quantified using inductively coupled plasma optical emission spectroscopy (ICP-OES, Agilent 5900 SVDV) after microwave digestion using HNO_3 and filtration through 0.45 μm membranes.

Residual alkali. The residual alkali concentration in the spent liquor from the soda cooking was quantified using a modular OMNIS professional titrator (Metrohm, Switzerland) equipped with LL-Unitrode WOC pH electrode, in accordance with SCAN-N 33:94.

Separation efficiency. The fractionation efficiency of the ultrafiltration was assessed by determining the molecular weight distributions (MWD) of the retentate and permeate via gel permeation chromatography (GPC). Prior to injection, the liquid fractions were lyophilized and subsequently

View Article Online
DOI: 10.1039/D6GC01257D

reconstituted in 0.1 M NaOH to achieve a final concentration of 1–2 mg/mL. Next, the solutions were subjected to mild sonication and passed through 0.45 µm PTFE syringe filters to ensure homogeneity and particulates removal. Chromatographic separation was performed on an Agilent 1100 Series system (USA) tailored for alkaline lignin characterization. Data acquisition and Mw calculations were executed using the ChemStation GPC data analysis suite.

GC-MS. The qualitative and semi-quantitative profile of low-molecular-weight organic constituents in bagasse (B), pretreatment liquids (B-P1), soda liquor (B-P1-P2) and its ultrafiltration fractions (feed, permeate and retentate), along with the hydrolysates prepared for HexA determination were established using Gas Chromatography-Mass Spectrometry (GC-MS; Shimadzu QP2010SE, Japan). Prior to analysis, silylation was implemented to enhance the volatility of the analytes. Sample derivatization was performed by solubilizing aliquots in 500 µL of pyridine spiked with tetracosane (1 mg/mL) as the internal standard. This was followed by the addition of 300 µL of BSTFA. The reaction mixture was then subjected to a two-phase thermal incubation at 70 °C (initially for 5 min, followed by 40 min), the intermittent vortex agitation was applied in between each step. Chromatographic separation was carried out on an HP-5 capillary column (30 m x 0.25 mm (i.d.), 0.25 µm film thickness) via an Optic 4 injector operating in split mode (1:10) at 300 °C. The column temperature was programmed with the following gradient: an initial hold at 80 °C for 5 min, a ramp of 4°C/min to 300 °C and hold for 20 min. Quantitative values were calculated based on the peak area ratio relative to the C24 internal standard, with all measurements performed in single unless otherwise explained. The mass spectra were compared with those from authentic compounds [A], available databases (including Organic Acids Library (TMS-oxime) (asahikawa-med.ac.jp) [J], NIST Chemistry WebBook [N]), and literature data.[10,17-19]

Acid precipitates "lignin" and NMR analysis. Lignin (or acidic precipitate) fractions were recovered from the soda spent liquor (feed), retentate and permeate. 20% (w/w) sulfuric acid (H_2SO_4) was added dropwise to 50 mL of the liquid under constant magnetic stirring. The acidification process included an equilibration step (30 mins stabilization) when pH reached 5.0, and then it is further reduced to 2.5 to ensure a complete precipitation of "lignin". The precipitated "lignin" was recovered by centrifugation at 10,000 rpm for 10 mins. Next, the crude "lignin" pellet was resuspended and washed repeatedly with deionized water until the supernatant pH stabilized between 3.5 and 4.0. Finally, the purified lignin was subsequently freeze-dried and reconstituted in a deuterated solvent system comprising DMSO-d_6 and pyridine-d_5 (4:1, v/v) using a Bruker AV NEO 400 MHz spectrometer (Germany). For the heteronuclear single quantum coherence (HSQC), the spectral windows were defined as 10 ppm for the proton (^{1}H) dimension and 200 ppm for the carbon (^{13}C) dimension. Data acquisition utilized a matrix of 1024 complex points in the direct dimension and 128 increments in the indirect dimension, with 64 scans accumulated per increment to optimize the signal-to-noise ratio. Chemical shifts were calibrated against the solvent peak of DMSO-d_6 (δH=2.49 ppm; δC= 39.5 ppm). All spectrums were processed using TopSpin 4.4.0 software and assigned following literatures.[20,21]

Results and discussion

Effects of pretreatment, pulp characteristics, and silica migration

To evaluate the efficiency of pretreatment in removing non-structural components from bagasse, chemical profile of raw material extracts (DCM- and acetone-soluble) and pretreatment (B-P1, **Table S1**) liquid were characterized using GC-MS **(Fig. 2 and Table S2)**. Analysis indicates that the lipophilic components of bagasse primarily consist of three major classes: long-chain fatty acids, fatty alcohols, and sterols. As depicted in **Fig. 2**, multiple prominent characteristic peaks appeared in the chromatogram, corresponding to the high-abundance compounds that are summarized in **Table S2**. First, within the fatty acid fraction, palmitic acid (C16:0), oleic acid (C18:1), and stearic acid (C18:0) were identified as major constituents, consistent with the previous findings.[22] A fatty acid mixture

derived from sugarcane wax oil exhibited anti-inflammatory activity in inflammatory models.[23] However, the long-chain fatty acids and fatty alcohol fraction of 1-octacosanol (C28:0) are not observed from the pretreatment liquor using water (B-P1) and mild alkali (B-P1-P2). High presence of 1-octacosanol in the bagasse holds significant health benefits.[24,25] β-Sitosterol is another significant extractive present at acetone-soluble fraction. Beyond β-Sitosterol, campesterol and stigmasterol were identified in the acetone extract, a composition consistent with findings by supercritical CO_2.[22]

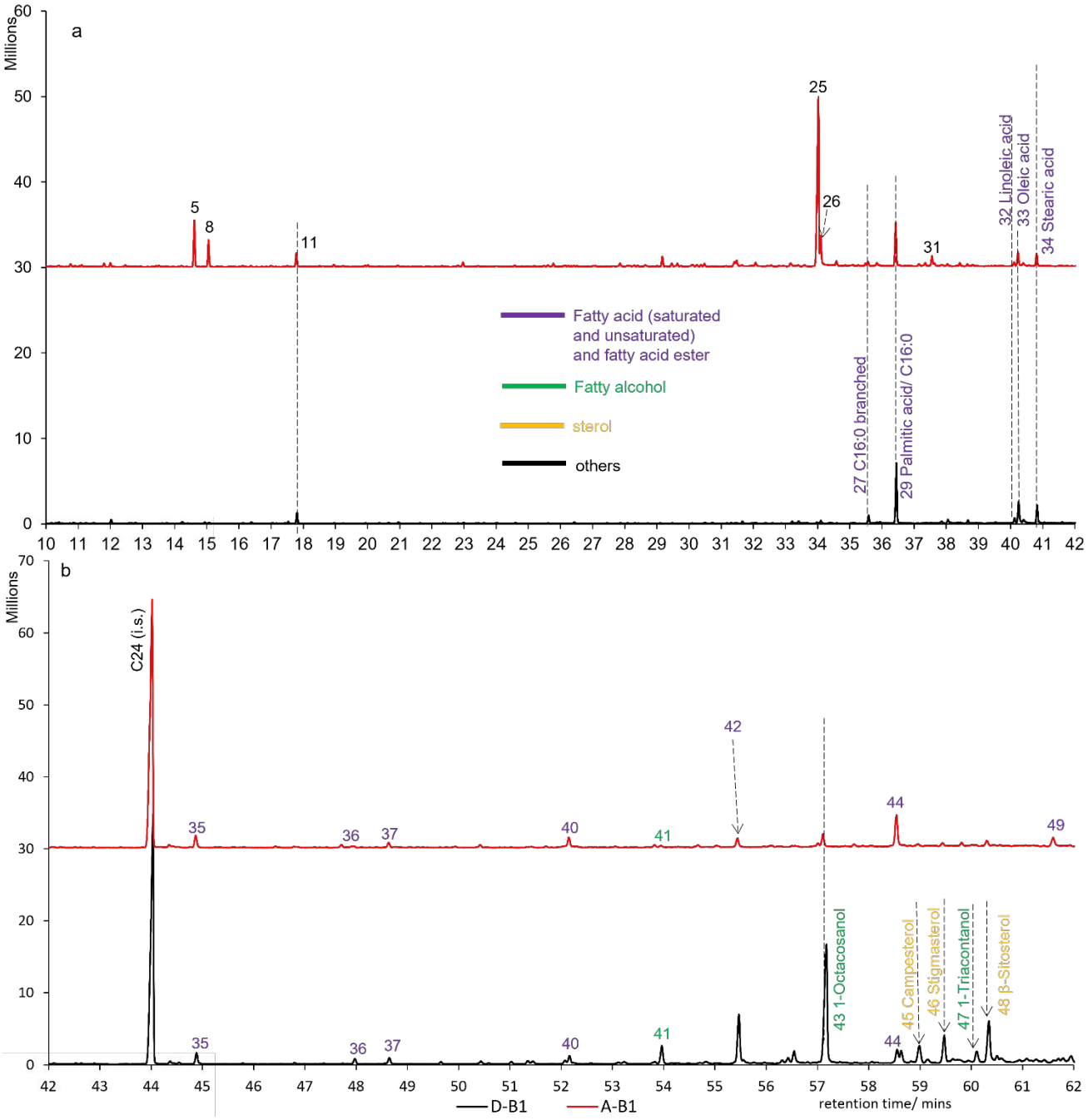

Fig. 2 GC-MS total-ion chromatogram of bagasse showing major peaks along with the internal standard (C24, i.s.) for dichloromethane- (D-B1) and acetone- (A-B1) extractables at retention time: **a** 10-42 min; **b** 42-62 min. More detailed assignments and codes are summarized at **Table S2**.

GC-MS spectra of the pretreatment samples revealed significant differences in chemical selectivity between B-P1 and B-P1-P2 (**Fig. 3**). B-P1 primarily removed water-soluble extracts from the fibrous bagasse. The dominance of glucose and disaccharide in the chromatogram (**B-P1, Fig. 3**) indicates that mild water washing served to wash out mainly free sugars. Citric acid[26], lactic acid[27] and glutamic

View Article Online
DOI: 10.1039/D6GC01257D

acid[28], are known organic acids, that can be generated by microbial fermentation of bagasse. The identification of other amino acids (such as L-Isoleucine and phenylalanine) is essential amino acids act as precursors in biological pathways of protein taking place during the storage of the bagasse. In contrast to B-P1, the B-P1-P2 solution exhibited different characteristics, most notably the substantial release of 4-coumaric acid and ferulic acid. This saponification phenomenon provides molecular-level hypothesis for the mechanism of mild alkaline treatment, which breaks possibly the intermolecular ester bonds linking hemicelluloses and lignin.[29] Our data confirms that B-P1-P2 suffices to cleave these alkali-labile ester bonds, releasing bound phenolic acids that are possibly linked into the main structural lignin-carbohydrate matrix. Furthermore, the detection of HAs such as xyloisosaccharinic acid (XISA) and 3-deoxypentonic acid indicate partial alkali degradation (peeling reaction) of hemicelluloses.[9]

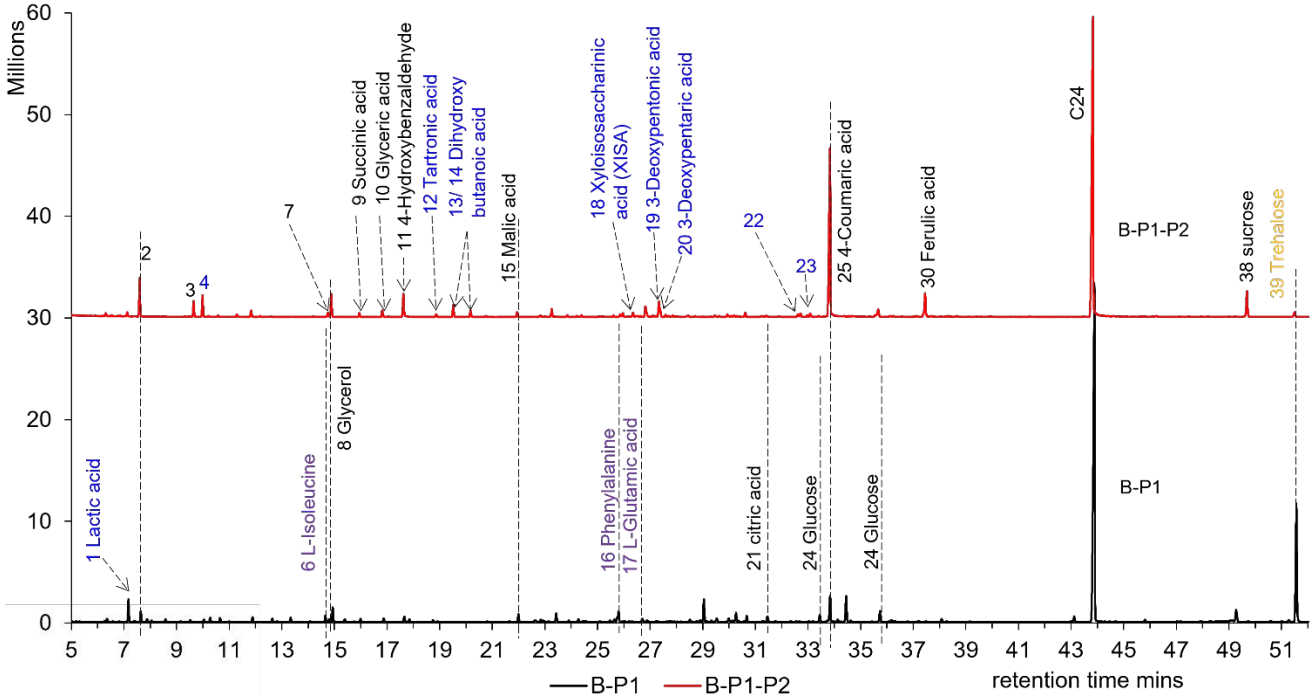

Fig. 3 GC-MS total-ion chromatogram of bagasse pretreatment liquids showing major peaks along with the internal standard (C24) at retention times 5-52 min: **a** B-P1 (water treatment); **b** B-P1-P2 (alkali pretreatment). Color codes for the hydroxy acids and amino acids: blue (hydroxy acids); purple (amino acids); black (rest). More detailed assignments, codes, and quantitative profile are at **Table S2**.

SEM was employed to visualize the structural evolution of bagasse fibers throughout the process. High-resolution imaging (**Fig. 4a and b**) revealed dense clusters of sub-micron spherical particles and amorphous deposits adhering to the surfaces of the fibrous bagasse. These observations are consistent with the presence of pith residues and waxy layers commonly reported in raw bagasse.[30] These surface impurities may form a recalcitrant physical barrier that can hinder the penetration of cooking chemicals. As depicted in **Fig. 4** (c->d), while the fiber bundles remained structurally intact after removal of the spherical "granule", the surface appeared much cleaner and polished. The bundles (**Fig. 4e->f**) were successfully delignified into fibers. The resulting pulp exhibited a characteristic flat, ribbon-like morphology with a collapsed lumen, typical of chemically delignified non-wood fibers. The FS5 analysis (**Table S3**) yielded a fiber length of 1.66 mm, a width of 21.0 μm, and a curl index of 7.9%. These values are consistent with those reported previously,[1] indicating that the soda cooking effectively separated the fibers while preserving their natural length.

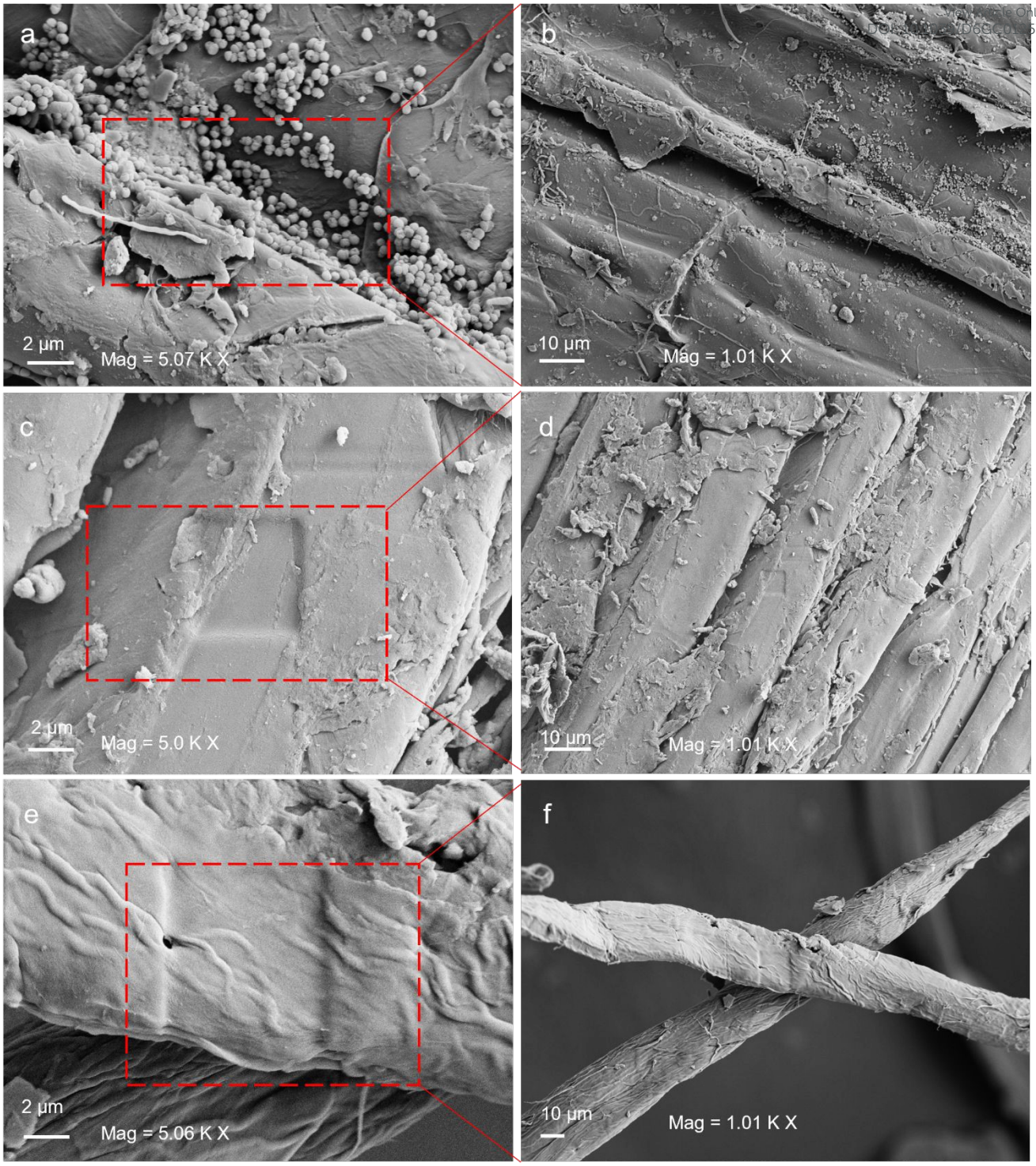

Fig. 4 SEM imaging at increasing magnification of fibrous bagasse B (a->b); hot water-washed bagasse (B-P1) (c->d); cooked pulp (B-P1-P2-C) (e->f). More detailed SEM images are summarized at **Figs. S1-S3**.

Although alkaline pretreatment using 0.1M NaOH was originally designed to liberate amorphous phytoliths into soluble sodium silicate (Na_2SiO_3) for desilification,[31] relative silicon content even surprisingly fluctuated from fibrous bagasse to the pulp (B-P1-P2-C) after the mild alkali treatment as shown at **Fig. 5a**. The hypothesis about silicon migration appears speculative and is supported by direct surface or bulk characterization using multiple analytical techniques, including SEM-EDX, XRD, and XPS (**Fig. 5b-d and Fig. S4-S6**). XRD analysis reveals distinct diffraction hump at ~29.42°

View Article Online
DOI: 10.1039/D6GC01257D

attributed to poor crystallinity of calcium-silicate[32]. A diffraction peak at ~26.73° (2θ) is more commonly attributed to crystalline inorganic phases of the acetone-soluble extracts out of ground-form bagasse pulp. The enhancement of cellulose intensity at B-P1-P2-C (**Fig. S6b**) is attributed to removal of amorphous acetone-soluble extractives components. Calcium silicate, as the primary form of silica, is also justified from top 2-3 nm of B-P1-P2-C (ground form, post-extracted) using XPS. A single component of Si was found in the Si 2p region, with the 2p3/2 peak located at approximately 102.5 eV, which is a typical energy for silicates. Likewise, a single component was found in the Ca 2p region with the 2p3/2 peak located at approximately 347.4 eV. This is most likely also related to calcium in a silicate. There are almost equal amounts of Ca (0.27 %) and Si (0.34 %) in the sample, while only trace amounts of sodium (0.01 %) could be detected (binding energy approximately 1071.5 eV). Calcium silicate ($CaSiO_3$) is found from one spot out of SEM-EDX analysis of B-P1-P2-C pulp sheet along with other multiple forms silicon dioxide (SiO_2), aluminosilicate, magnesium silicates. To conclude, our hypothesis is that highly- reactive Ca^{2+} rapidly displaces Na^{+} under the cooking condition and reacts *in situ* with SiO_3^{2-}, explaining the unexpected surge in calcium content at B-P1-P2-C in **Fig. 5a**, the dissolved silica (out of B-P1-P2) was not leached away but instead “captured” first by sodium at B-P1-P2 before the sodium-calcium exchange, the calcium silicate ($CaSiO_3$) is then reprecipitated back to the fiber surface of B-P1-P2-C potentially limiting the delignification rate of the soda cooking.

View Article Online
DOI: 10.1039/D6GC01257D

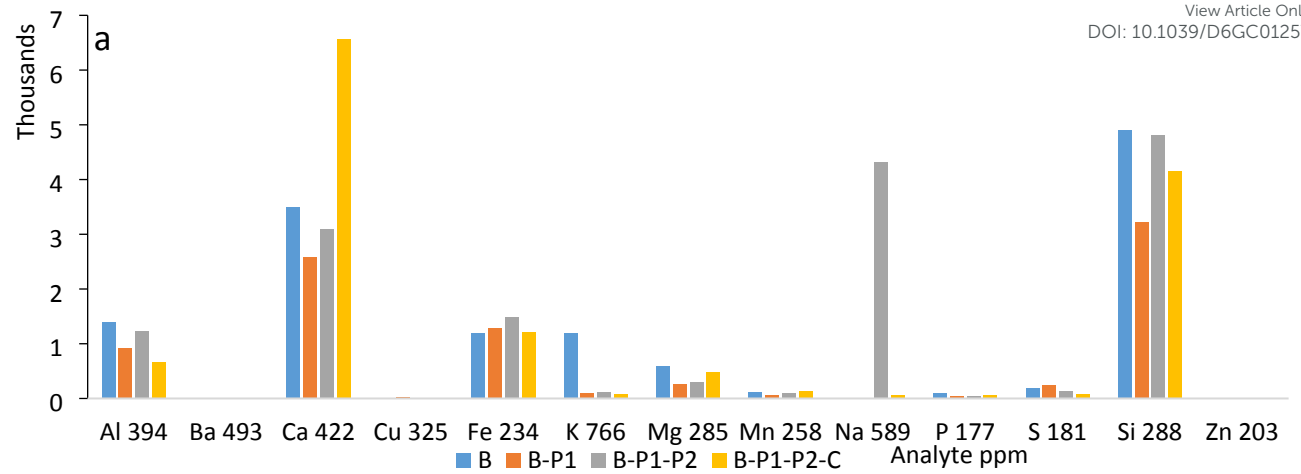

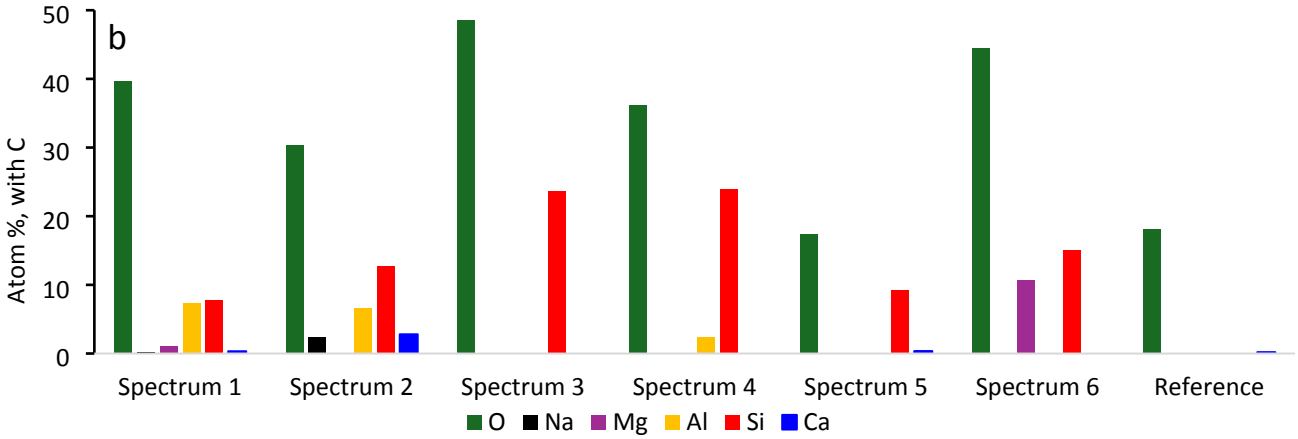

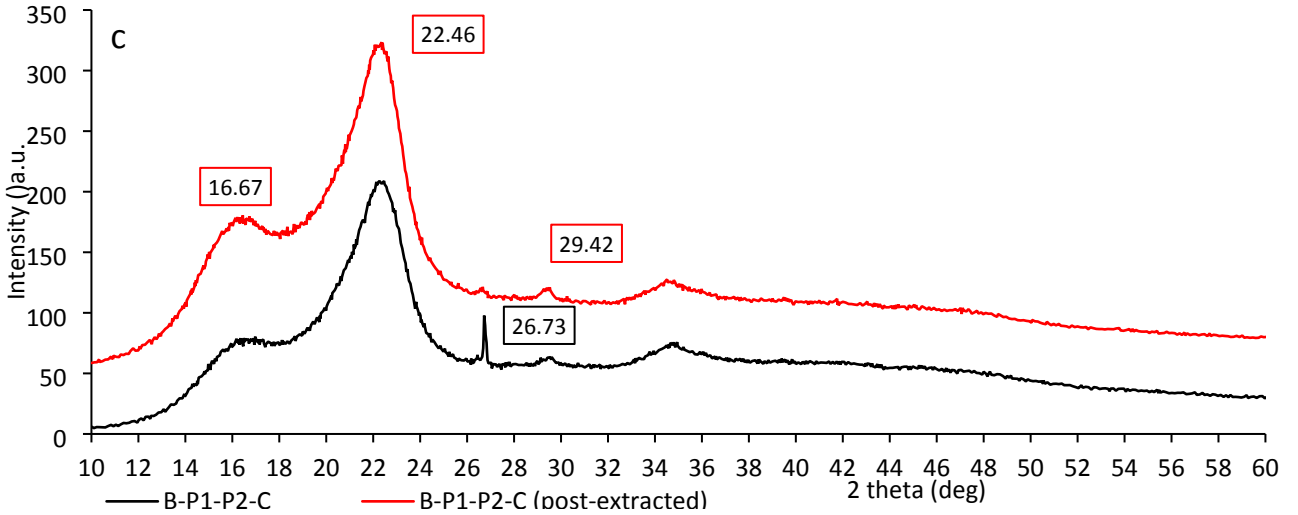

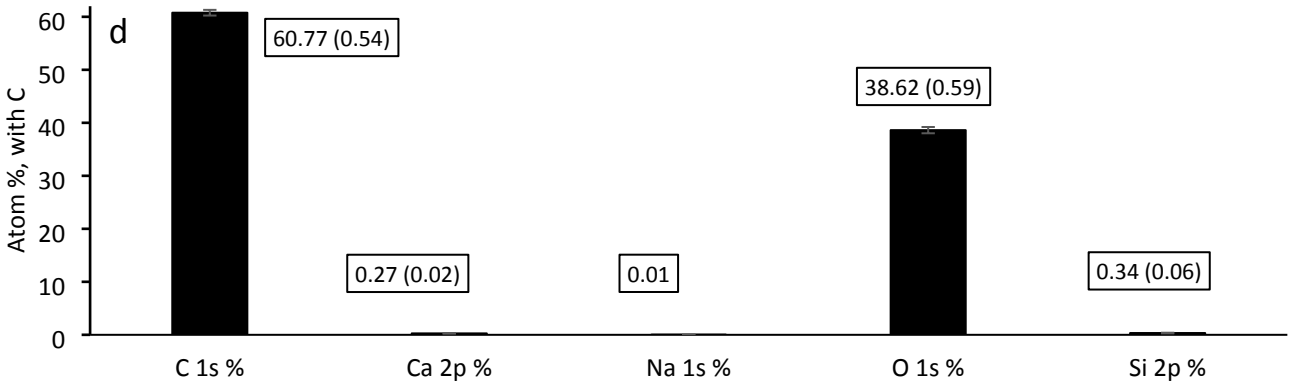

View Article Online
DOI: 10.1039/D6GC01257D

Fig. 5 Inorganic compositional analysis by multiple techniques: **a** ICP-OES analysis of multiple samples (fibrous bagasse (B); water pretreated bagasse (B-P1); alkali washed bagasse (B-P1-P2); soda cooking pulp (B-P1-P2-C)); **b** SEM-EDX analysis of B-P1-P2-C paper sheet (**Fig. S12**) based on six spectrum positions (**Fig. S4**) in comparison to reference spot (pulp cellulose fiber); **c** XRD patterns of B-P1-P2-C in comparison to its post-extracted form (B-P1-P2-C (post-extracted)); **d** XPS analysis of (B-P1-P2-C (post-extracted) showing relative concentrations of the elements (STD is included as part of the parenthesis) averaged from all three positions on the sample surface. More detailed results are summarized at **Fig. S4-S6**.

A-stage on hexenuronic acid removal

The standard UV protocol[15] was originally designed for hardwood kraft pulps, which typically contain high HexA levels (often >40–60 meq/kg). In such samples, the HexA derived signal is strong, making background interference negligible. However, the bagasse in this study has a relatively low initial HexA content (14.4 meq/kg), the unbleached pulp spectrum displays a broad background absorption instead of a sharp peak at 245 nm, characteristics of the absorption maximum for 2-furoic acid (**Fig. S7**). However, the baseline is not flat and there is no clear absorption band associated with 2-furonic acid at A245 (absorbance at 245 nm) for hydrolysate of both D0 pulp and ADO pulp. GC-MS (**Table S4 and Fig. S8-S9**) is thus applied for both qualitative and semi-quantitative analysis of 2-furonic acid from the same hydrolysate prepared for the UV protocol. The detected 2-furonic acid content from hydrolysate of unbleached pulp (0.59 mg/g) is roughly 5-10 times higher than that from D0 pulp (0.05 mg/g) and A/DO pulp (0.14 mg/g), respectively. Consequently, applying this wood-based method to bagasse likely overestimates the real HexA content to some extent, however this potential limitation on calculation of HexA removal rate has been limited because residual HexA (or 2-furonic acid) content is extremely low regardless of the methods. HexA content calculation using the standard UV protocol is applied for the follow up discussion.

Normally mass loss associated with A-stage can be primarily attributed to the selective degradation of hemicelluloses and HexA removal, as evidenced by the relatively lower content of xylose in A/D_0 (**Fig. 6 and Table S5**) in comparison to D_0. However, A-stage brings negligible yield loss from A/D_0 to D_0, attributed possibly to the relatively higher kappa at A/D_0 pulp. 14.4 meq/kg HexA of bagasse is consistent with 16.5 meq/kg that was reported previously. Following A/D_0 sequential treatment,[2] HexA content significantly decreased to 7.4 meq/kg (**Table 2**), representing almost half removal of HexA. In contrast, the control D_0 retained a higher HexA residue of 8.8 meq/kg. This difference reveals the impact when including the A-stage (pH 3.5 and 95°C), the glycosidic bonds linking HexA to the xylan backbone undergo selective acid hydrolysis for converting HexA into furan derivatives (e.g., 2-furanoic acid), which are then discharged with wash water, thereby preventing its entry into subsequent oxidation stages and further impact on brightness reversion and ClO_2 consumption.[7] The A/D_0 sequential process, benefiting from the prior removal of HexA, achieved 59% lignin removal (kappa reduced from 11.7 to 4.8) with only 2.0% ClO_2 dosage, equivalent to a 63% delignification rate (kappa from 8.7 to 3.1) with 2.5% ClO_2 dosage based on D-hot process reported previously.[2]

View Article Online
DOI: 10.1039/D6GC01257D

Table 2 Pulps' properties of bagasse treated with A/D_0-E_p-D_1 (4% Act. Cl) in comparison to D_0-E_p-D_1 (5.2% Act. Cl): kappa; viscosity; ISO brightness; HexA content. Photographs of the pulp are included at **Fig. S10**. STD is included in the parenthesis and error bars are displayed at **Fig. S11**. n.a. refers to not applicable.

	Kappa		Viscosity (ml/g)		Brightness (ISO %)		HexA (c, meq/kg)		Yields (%)	
	A/$D_0E_pD_1$	$D_0E_pD_1$	A/$D_0E_pD_1$	$D_0E_pD_1$	A/$D_0E_pD_1$	$D_0E_pD_1$	A/$D_0E_pD_1$	$D_0E_pD_1$	A/$D_0E_pD_1$	$D_0E_pD_1$
Unbleached	11.7 (0.005)		1029 (1)		39 (0.4)		14.4 (0.03)		45.7	
A/D_0 (D_0)	4.8 (0.001)	4.4 (0.01)	949 (5)	1012 (3)	47 (1.4)	56 (0.4)	7.4 (0.1)	8.8 (0.1)	44.7	44.3
E_p	3.1 (0.02)	2.8 (0.01)	734 (10)	918 (9)	60 (0.6)	69 (0.3)	n.a.	n.a.	n.a.	n.a.
D_1	0.5	0.5	685 (3)	874 (3)	75 (0.7)	80 (0.3)	n.a.	n.a.	n.a.	n.a.

Due to the effective HexA reduction when A-stage was implemented, A/D_0-E_p-D_1 achieves a 25% reduction in total active chlorine usage from 5.2% to 4.0% despite a compromise of losing 21% viscosity (**Table 2)**. In specific, the viscosity reduction of 7.8% in this A/D_0 process (1029 ml/g to 949 ml/g) is comparable to the ~8.4% decrease (1095 ml/g to 1003 ml/g) in the D-hot process reported previously.[2] Raw bagasse exhibits typical non-wood biomass characteristics, with a lignin content of approximately 20–25%, consistent with the composition reported earlier for bagasse (~45% cellulose, ~28% hemicellulose, ~22% lignin).[1] The detailed sugar profile in **Fig. 6** reveals the specific impact of the A-stage on hemicelluloses components (primarily xylan). A slight decrease in xylose content was observed from 24.2 % (D_0-E_p-D_1) to 23.9% (A/D_0-E_p-D_1). Acidic conditions (pH 3.5, 95°C) inevitably induce partial hydrolysis of short-chain amorphous xylans while attacking HexA glycosidic bonds.[4,7] Overall, moderate removal of xylan side chains not only eliminates roughly 50% of HexA but also reduces the risks behind AOX generation and brightness reversion during subsequent bleaching. Thus, the slight decrease of xylose from D_0-E_p-D_1 pulp to A/D_0-E_p-D_1 pulp (**Table S5)** aligns to the effect originating from A-stage**.**

View Article Online
DOI: 10.1039/D6GC01257D

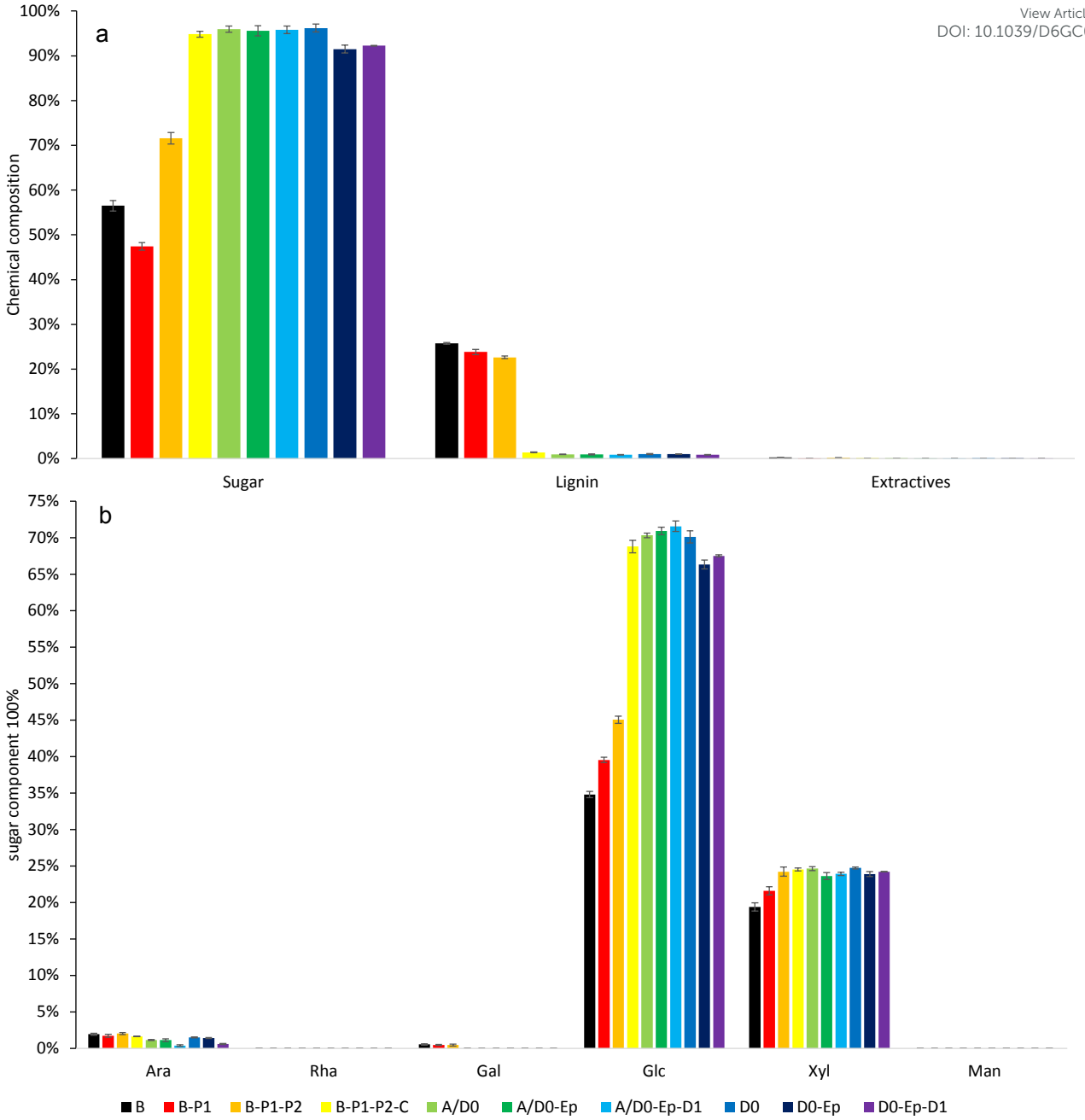

Fig. 6 Overall chemical composition (a) and carbohydrate composition (b) (% of anhydrosugars in the original dry mass without yield consideration) from the fibrous bagasse (B, **Table S1**) to the bleached pulp. The relative composition is displayed at **Table S5**. Abbreviations: Arabinose (Ara), rhamnose (Rha), galactose (Gal), glucose (Glc), xylose (Xyl), mannose (Man).

Fiber viscosity, as an indicator of cellulose molecular weight, influences primarily fiber strength; however, the relationship to paper strength is indirect and tensile strength properties are moderated also by fiber morphology (coarseness, aspect ratio) and inter-fiber bonding (that adheres the fibers together in the paper matrix) as failure typically occurs at fiber–fiber interfaces rather than within the fibers themselves. Effect of pulp viscosity on tensile strength properties of bagasse pulp fiber is conducted for pulps having lower viscosity (A/D0 949 ml/g and A/D0EpD1 685 ml/g, **Table 2**) in comparison to the pulps without A-stage treatment (D0 1012 ml/g and D0EpD1 874 ml/g, **Table 2**), respectively. Roughly 5% (28.88 -> 27.56) and 12.6% (30.4-> 26.6) loss of tensile index was seen in relation to 6.2% and 21.6% loss of viscosity from D0-> AD0 pulp and D0EpD1-> A/D0EpD1 pulp, respectively. (**Table S6 and Fig. S12-S14**) No visible differences have been seen from the Young

View Article Online
DOI: 10.1039/D6GC01257D

modulus (**Table S6**). Moderate level of 21.6% loss in viscosity results in proportional but not linear reductions in tensile strength of their respective sheet. This observation is also supported by the reference statement about losing the cellulose DP would negatively affect the paper strength only when reaching threshold level for sulfate pulp of softwood (15 to 20 mPa·s (or 800 to 915 mL/g intrinsic viscosity))[33] and bamboo (8 mPa·s)[34]. In this scenario, bagasse fiber has most extensive application in the manufacturing of molded pulp food-service packaging and disposable tableware. In molded pulp food-service packaging, bagasse fibers do not require high tensile strength, as the primary mechanical demands involve compression, bending, and wet stability rather than tensile loading.

Ultrafiltration

The two-dimensional HSQC NMR spectrum (**Fig. 7)** reveals the impact of ultrafiltration on the chemical structure of lignin at the atomic level from retentate and permeate in comparison to feed. First, the behavior of the dominant inter-unit linkages, particularly β-O-4 aryl ethers (substructure A), offers a direct insight into the depolymerization extent.[21] In the spectrum of both retentate and feed, the signals for Cα–Hα (Aα), Cβ–Hβ (Aβ), Cγ–Hγ (Aγ) correlations in β-O-4 linkages are seen at δ_C/δ_H of 71.52/5.03, 86.28/4.15, and 61.69/3.58 ppm, respectively. Furthermore, xylan (Xyl) with Xyl-1, Xyl-2, Xyl-3, Xyl-4, and Xyl-5 (in red, **Fig. 7**) correlations at δC/δH of 101.6/4.38, 72.5/ 3.21, 73.8/3.41, 75.2/3.65 and 63.2/3.98 (3.27) ppm, respectively, were present both in feed and retentate however not in permeate (**Fig. 7c**). Given that the ultrafiltration membrane used in this study has a MWCO of only 0.5 kDa, free monosaccharide xylose should theoretically readily penetrate through the membrane pores into the permeate. However, xylan was retained in high proportions within the retentate, strongly indicating that these carbohydrates do not exist in free form at feed and retentate as well as permeate (**Fig. 9**). Instead, they are possibly covalently bound to lignin, forming stable lignin-xylan complexes.[35,36]

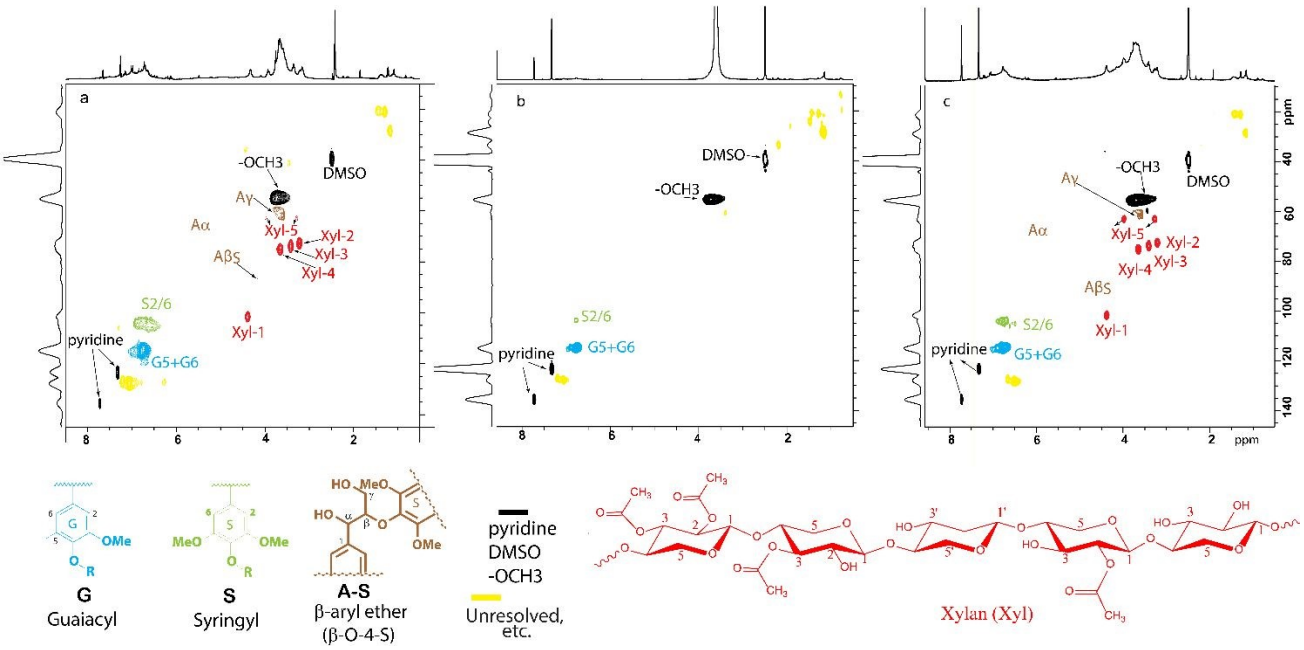

Fig. 7 Both aromatic and side chain (δ_C/δ_H, 10–145/0.5–8.5 ppm) regions of $^1H–^{13}C$ HSQC NMR spectrum of acid precipitates "lignin" in 0.8 ml DMSO-d_6/ pyridine-d_5 (v/v, 4/1) from multiple sources: **a** feed (51.03 mg); **b** permeate (5.86 mg); **c** retentate (5.29 mg).

The efficacy of the ultrafiltration in fractionating high MW lignin-xylan complex based on hydrodynamic volume was confirmed by GPC (**Fig. 8 and Table S7**). The parent spent liquor (feed) exhibited a broad MW distribution (weight-average molecular weight (M_w) ≈ 2776 g/mol, number-average molecular weight (M_n) ≈ 641 g/mol), typical of soda lignin containing a heterogeneous mixture of

View Article Online
DOI: 10.1039/D6GC01257D

degraded fragments. The retentate fraction was significantly enriched in high MW species, with its M_w increasing to 4032 g/mol, representing a ~45% increase compared to feed. Conversely, the permeate contained only oligomeric fragments with a much lower M_w of 840 g/mol. This stark contrast (4.8 times) proved again the 0.5 kDa-sized membrane effectively retained the macromolecular lignin-xylan complex in the retentate while allowing smaller phenolic oligomers (sugars, HAs, and alkali) to pass through membrane as part of permeate. 1.97 g NaOH/L of residual alkali was detected from the spent liquor, suggesting that the free-form alkali has been mostly consumed in the cooking, the significant abundance of Na^+ (possibly primarily Na_2CO3) at feed and retentate (**Fig. S15**) implies that alkali recovery can be positively achieved through multiple cycles of ultrafiltration prior the causticizing step for alkali recovery (**Fig. 1b**). Permeate (water flux) dropped progressively (roughly 29%) from 0.42 L/m²h (cycle 1, **Fig. S16**) to 0.36 L/m²h (cycle 2) and further down to 0.30 L/m²h (cycle 1) indicates a consistent rate of membrane fouling during each operating cycle.

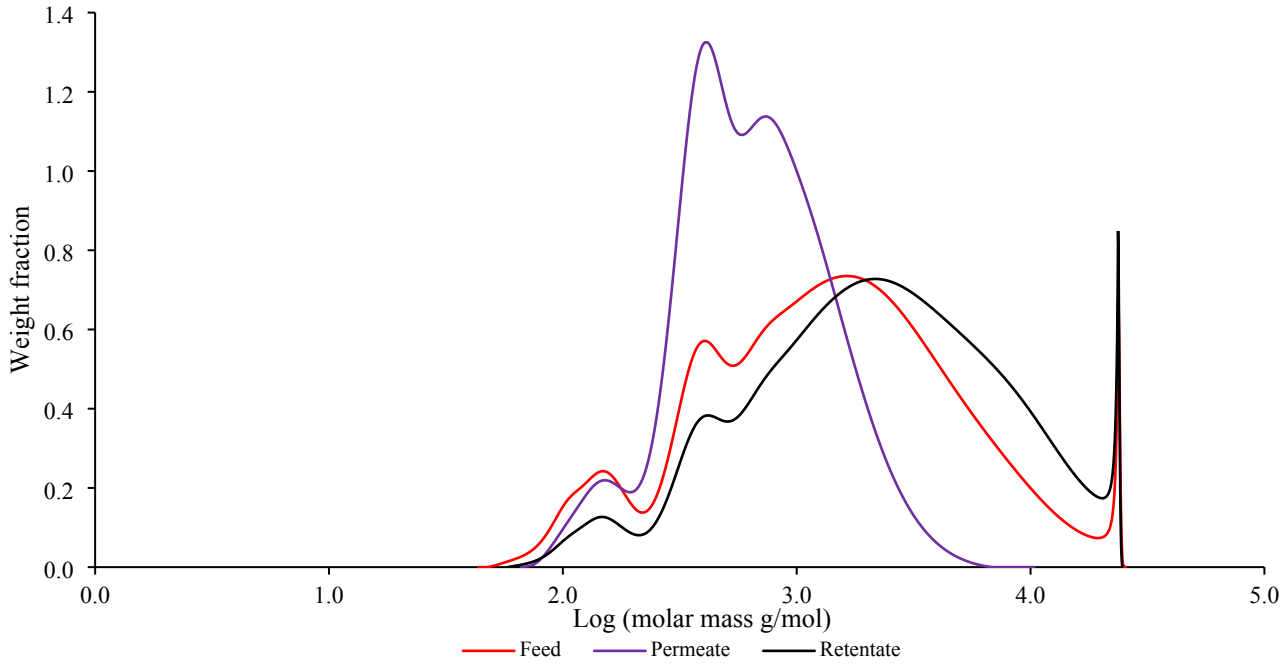

Fig. 8 The elution profile of different lignin sources derived from the ultrafiltration (i.e. black liquor; permeate; and retentate) from MALLS-SEC. More detailed information is summarized at **Table S7**.

GC-MS characterization of low MW components in the multiple sources of liquid revealed a complex profile of aliphatic HAs. As shown in **Fig. 9**, significant HA signals were detected in both the feed and permeate, with their structures further confirmed by mass spectrometry fragmentation patterns (**Fig. S17**). Among the detected compounds, lactic acid, glycolic acid, and 2-hydroxybutanoic acid (2-HBA) were identified as the major aliphatic acid components (**Table S8**). The formation of these HAs is attributed to the "peeling reaction" of polysaccharides during alkaline pulping. The reducing ends of cellulose and hemicelluloses are highly-unstable under thermal-alkali conditions, undergoing stepwise degradation and rearrangement to form various HAs.[9] Notably, xyloisosaccharinic acid (XISA) (rt 26.37 min, **Fig. 9**), a major degradation product formed over the alkaline hydrolysis of hemicelluloses, is also identified.[10] Semi-quantitative analysis (**Table 3**) indicates that an overall recovery rate of 72% HAs is achieved in the permeate, for example lactic acid and 2-HBA in the permeate (0.18 g/L and 0.17 g/L, respectively) were significantly higher than those in retentate (< 0.04 g/L). Similar observations have demonstrated ultrafiltration as a key step in black liquor fractionation out of chemical pulping process of softwood, retaining over 90% of lignin in the retentate to yield a pure permeate stream rich in HAs and alkali.[12,37]

View Article Online
DOI: 10.1039/D6GC01257D

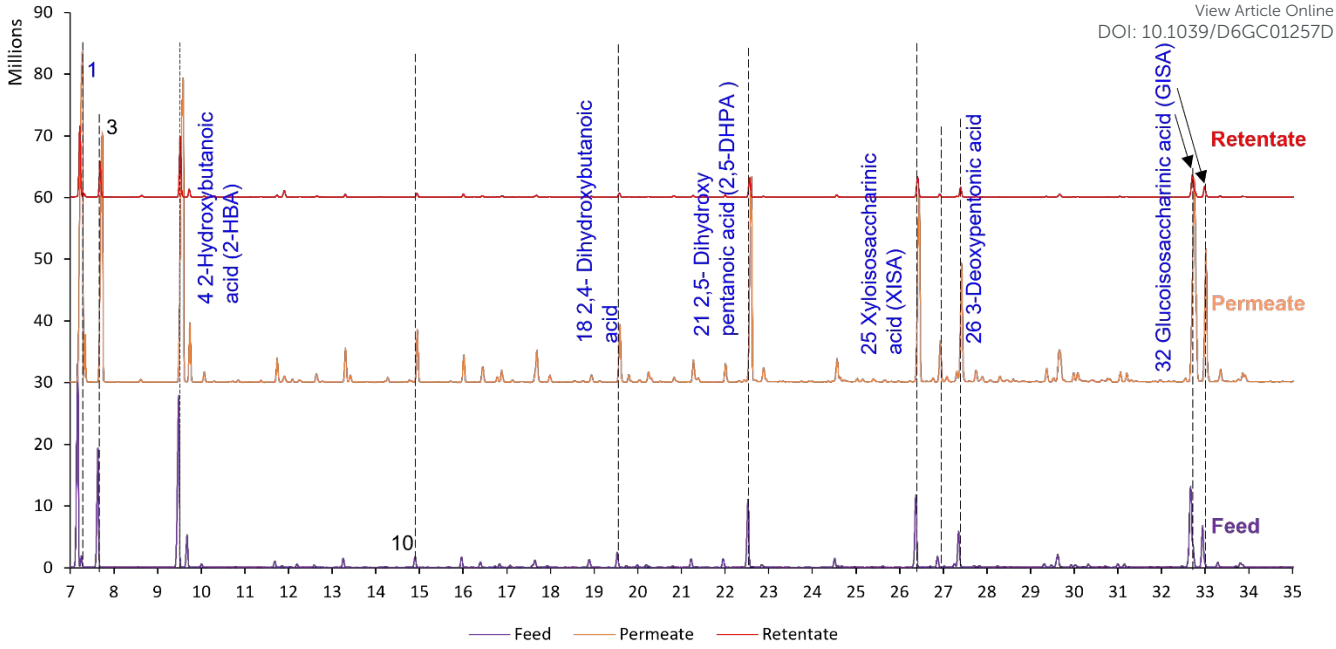

Fig. 9 GC-MS total-ion chromatogram of multiple sources of spent liquor after ultrafiltration showing major peaks along with internal standard (C24, Std) at retention times 7-33 min: **a** feed; **b** permeate; **c** retentate. Color codes for hydroxy acids is blue. More detailed assignments and number codes are at **Table S8**. Mass spectrums of some classic hydroxy acids are summarized at **Fig. S17**.

Table 3 Overall content (in g/L) of the hydroxy acids at spent liquor (feed), permeate as well as retentate. The complete profile and codes of the assignment are summarized at **Table S8**.

Code	Ret time, mins	Compounds	Feed	Permeate	Retentate
1	7.167	Lactic acid	0.275	0.180	0.035
2	7.633	Glycolic acid	0.145	0.110	0.016
4	9.482	2-Hydroxybutanoic acid	0.245	0.167	0.030
5	9.676	Oxalic acid	0.040	0.017	0.003
8	13.255	4-Hydroxybutanoic acid	0.012	0.010	0
11	15.965	Succinic acid	0.013	0.008	0
12	16.402	Methylsuccinic acid	0.004	0.002	0
18	19.529	2,4-Dihydroxybutanoic acid	0.021	0.017	0.001
21	22.526	2,5- Dihydroxy pentanoic acid (2,5-DHPA)	0.096	0.080	0.010
23	24.514	2-Hydroxyglutaric acid	0.012	0.005	0
25	26.372	Xyloisosaccharinic acid (XISA)	0.105	0.084	0.010
26	26.867	3-Deoxy-erythro-pentonic acid	0.015	0.013	0.002
27	27.252	2-Hydroxyadipic acid	0.005	0.002	0
28	27.353	3-Deoxy-threo-pentonic acid	0.049	0.036	0.004
32	32.665	Glucoisosaccharinic acid (GISA)	0.134	0.102	0.011
33	32.706	3-Deoxy-arabino-hexonic acid	0.025	0.019	0
32	32.940	Glucoisosaccharinic acid (GISA)	0.061	0.048	0.005
35	33.291	3-Deoxy-2-hydroxymethyl-erythro-pentaric acid	0.006	0.003	0
37	33.858	3-Deoxy-2-hydroxymethyl-threo-pentaric acid	0.002	0.002	0
	Overall		1.266	0.907	0.127
	HA recovery%			72	10

For the first time, implementing ultrafiltration at bagasse recovery process opens promise of multiple recovery of sugar-degradation HAs along with alkali and lignin-xylan complex from spent liquor (**Fig. 1b**) Moreover, majority of sulfur compounds should already be removed at cooking plant via non-condensable gases (NCGs). The only sulfur-source that enters fiberline should be the one originating from raw biomass, thus the produced spent liquor will not contain any sulfur compounds. So, the role

View Article Online
DOI: 10.1039/D6GC01257D

of reduction reactions converting sodium sulphate (Na_2SO_4) into sodium sulphide (Na_2S) is not anymore required for the traditional recovery boiler. Necessary steam (energy) required for pulping can be achieved with a traditional power boiler instead of the specialized Tomlinson recovery boiler. A much smaller and financially more affordable alternative solutions like simplified membrane and power boiler unit is for the first time demonstrated for closing the alkali recovery cycle and meeting energy demand of bagasse mill to partially replace costly Tomlinson recovery boiler.

Conclusions

This study demonstrated an integrated biorefinery strategy for bagasse valorization, addressing the dual challenges of HexA interference prior bleaching and the inefficient recovery of silica-rich spent liquor. A-stage proved for the first time effective in selectively removing half HexA prior to bleaching for bagasse pulp. This targeted removal allowed for a 25% reduction in ClO_2 consumption within the ECF bleaching sequence along with a trade-off compromise in 21.6% viscosity reduction and 12.6% loss of tensile index of the sheet compared to the reference sequence, attributed possibly to the hemicelluloses degradation. Ultrafiltration utilizing a 0.5 kDa-sized membrane concentrated high-purity lignin-xylan complex in the retentate while enriching the permeate with 72% low-molecular-weight HAs, such as xyloisosaccharinic acid (XISA) and glucoisosaccharinic acid (GISA). Strong presence of calcium ion detected at bagasse pulp leads to the speculative hypothesis that highly active Ca^{2+} rapidly replaces Na^{+} completely (or partially) and reacts *in situ* with SiO_3^{2-} under soda cooking conditions, the silica got dissolved first from alkali pretreatment stage and was not leached out however being first "captured" by the sodium prior the sodium-calcium exchange. Subsequently, calcium silicate is again reprecipitated back to the surface of the fibers after cooking, reminding us of challenges behind silica control in the bagasse fiberline.

Future research avenues shall first establish a HexA detection method tailored for non-wood and prioritize optimizing the A-stage parameters, specifically tailoring acid charge and temperature, to achieve a better balance between bleaching chemical savings and pulp quality preservation. Additionally, downstream efforts should focus on fine-tuning membrane ultrafiltration to minimize fouling of membranes without compromise of flux rate (**Fig. S16**), multiple cut-off Mw membranes will also be investigated to improve the separation efficiency and shorten the filtration time. Mass balance of the HAs and alkali recovery (from permeate) along with recovery and application of lignin-xylan complexes (from retentate) will be more carefully investigated for establishing thermodynamic mass and energy balance[38] when in combined use with the traditional power boiler, thereby justifying the economic potential of partially replacing the costly Tomlinson recovery boiler (**Fig. 1b**).

Data availability

The authors declare that all the data that supports the findings of this study are available within the article and its ESI files or from the corresponding author upon reasonable request.

Conflicts of interest

There are no conflicts to declare.

Acknowledgements

The authors gratefully acknowledge the financial support provided by the Research Council of Finland under the project FACE+ (Grant No. 356520) as well as a donation grant from Andritz Oy to Aalto University Foundation. Additionally, the authors acknowledge the use of the research facilities in Bio 2 at Aalto University (Bioeconomy Infrastructure) for the experimental work. Besides, the authors express their gratitude to Prof. Tapani Vuorinen from Aalto University for his valuable inputs regarding the bleaching experiments and to Guilhermo Magalhaes from Andritz Oy for his conceptual contribution regarding the membrane fractionation approach. We also extend our sincere thanks to

View Article Online
DOI: 10.1039/D6GC01257D

Dr. Estefanía Isaza Ferro for her technical guidance and training regarding the ECF bleaching protocols. Furthermore, the invaluable expertise and assistance provided by Dr. Timo Pääkkönen concerning the operation of the Alfa Laval ultrafiltration system are highly appreciated. In addition, the assistance provided by Dr. Leena Pitkänen from Aalto University with GPC testing was invaluable. The authors also appreciate the coordination of bagasse delivery by Prof. Lei Wang (Westlake University, China) and Prof. Xueping Song (Guangxi University, China). Dr. Eero Hiltunen, Dr. Lassi Klemettinen, and Dr. Tewari Girish from Aalto University are appreciated for their support in tensile testing, SEM-EDX, as well as XRD when preparing for the reviewer's response.

Author contributions

Kun Ouyang: Investigation, Data Curation, Validation, Formal analysis, Writing - Original Draft. **Wajeeha Munib:** Investigation (Ultrafiltration); **Quang Le Huy:** Methodology, Investigation (Bleaching). **Lauri Leskinen:** Formal analysis (GC-MS); **Yue Wu:** Formal analysis (NMR); **Naveen Chenna:** Conceptualization, Resources, and Funding acquisition. **Inge Schlapp-Hackl:** Formal analysis (ICP-OES); **Jinze Dou:** Conceptualization, Methodology, Formal analysis, Visualization, Resources, Supervision, Project administration, Funding acquisition, Writing - Review & Editing.

References

1 M. S. Jahan, M. M. Rahman and Y. Ni, *Biofuels, Bioprod. Biorefin.*, 2021, **15**, 100–118, DOI: 10.1002/bbb.2143.

2 H. Zhang, S. Nie, C. Qin and S. Wang, *Ind. Crops Prod.*, 2019, **128**, 338–345, DOI: 10.1016/j.indcrop.2018.11.025.

3 D. Nguyen, X. Zhang, Z. H. Jiang, A. Audet, M. G. Paice, S. Renaud and A. Tsang, *Enzyme Microb. Technol.*, 2008, **43**, 130–136, DOI: 10.1016/j.enzmictec.2007.11.012.

4 A. A. Shatalov and H. Pereira, *Bioresour. Technol.*, 2009, **100**, 3069–3075, DOI: 10.1016/j.biortech.2009.01.020.

5 N. Mahadevan, N. C. Sridhar, P. N. Rao, K. Kalyanasundaram and A. R. K. Rao, *IPPTA*, 1986, **23**, 155–159.

6 A. Teleman, V. Harjunpää, M. Tenkanen, J. Buchert, T. Hausalo, T. Drakenberg and T. Vuorinen, *Carbohydr. Res.*, 1995, **272**, 55–71, DOI: 10.1016/0008-6215(95)96873-M.

7 T. Vuorinen, A. Teleman, P. Fagerström, J. Buchert and M. Tenkanen, *J. Pulp Pap. Sci.*, 1999, **25**, 155–162.

8 S. Nie, S. Wang, C. Qin, S. Yao, J. F. Ebonka, X. Song, and K. Li, *Bioresour. Technol.*, 2015, **196**, 413–417, DOI: 10.1016/j.biortech.2015.07.115.

9 P. Fardim, *Papermaking Science and Technology: Volume 6 Chemical pulping, Part 1: Fibre chemistry and technology*, Fapet Oy, Helsinki, 2011, pp. 216–217.

10 K. Niemelä and R. Alén, *Analytical Methods in Wood Chemistry, Pulping, and Papermaking*, Springer-Verlag, Heidelberg, 1999, pp. 193–231.

11 O. A. Ojelade, Q. Fu, S. Nair and C. W. Jones, *ACS Sustainable Chem. Eng.*, 2024, **12**, 9054–9066, DOI: 10.1021/acssuschemeng.4c00212.

12 J. Heinonen and T. Sainio, *Chem. Eng. Sci.*, 2019, **197**, 87–97, DOI: 10.1016/j.ces.2018.12.013.

13 A. Toledano, A. García, I. Mondragon and J. Labidi, *Sep. Purif. Technol.*, 2010, **71**, 38–43, DOI: 10.1016/j.seppur.2009.10.024.

View Article Online
DOI: 10.1039/D6GC01257D

14 C. A. E. Costa, P. C. R. Pinto and A. E. Rodrigues, *Sep. Purif. Technol.*, 2018, **192**, 140–151, DOI: 10.1016/j.seppur.2017.09.066.

15 M. Tenkanen, G. Gellerstedt, T. Vuorinen, A. Teleman, M. Perttula, J. Li and J. Buchert, *J. Pulp Pap. Sci.*, 1999, **25**, 306–311.

16 J. B. Sluiter, R. O. Ruiz, C. J. Scarlata, A. D. Sluiter and D. W. Templeton, *J. Agric. Food Chem.*, 2010, **58**, 9043–9053, DOI: 10.1021/jf1008023.

17 J. Dou, K. Niemelä, T. Haatainen, P. Tervola and J. Vehmaa, *J. Cleaner Prod.*, 2023, **405**, 136940, DOI: 10.1016/j.jclepro.2023.136940.

18 G. Petersson, *Tetrahedron*, 1970, **26**, 3413–3428, DOI: 10.1016/S0040-4020(01)92918-7.

19 G. Petersson, *Carbohydr. Res.*, 1975, **43**, 1–8, DOI: 10.1016/S0008-6215(00)83967-1.

20 J. Dou, H. Kim, Y. Li, D. Padmakshan, F. Yue, J. Ralph and T. Vuorinen, *J. Agric. Food Chem.*, 2018, **66**, 7294–7300, DOI: 10.1021/acs.jafc.8b02014.

21 J. C. del Río, A. G. Lino, J. L. Colodette, C. F. Lima, A. Gutiérrez, Á. T. Martínez, F. Lu, J. Ralph and J. Rencoret, *Biomass Bioenergy*, 2015, **81**, 322–338, DOI: 10.1016/j.biombioe.2015.07.006.

22 T. M. Attard, C. R. McElroy, C. A. Rezende, I. Polikarpov, J. H. Clark and A. J. Hunt, *Ind. Crops Prod.*, 2015, **76**, 95–103, DOI: 10.1016/j.indcrop.2015.05.077.

23 N. Ledón, A. Casacó, D. Remirez, A. González, J. Cruz, R. González, A. Capote, Z. Tolón, E. Rojas, V. J. Rodríguez, N. Merino, S. Rodríguez, O. Ancheta and M. C. Cano, *Phytomedicine*, 2007, **14**, 690–695, DOI: 10.1016/j.phymed.2006.12.019.

24 S. Feng, Z. Luo, F. Zeng, S. Liu, and Z. U. Khan, *Food Chem.*, 2015, **182**, 171–177, DOI: 10.1016/j.foodchem.2015.03.003.

25 J. C. Taylor, L. Rapport and G. B. Lockwood, *Nutrition*, 2003, **19**, 192–195, DOI: 10.1016/S0899-9007(02)00869-9.

26 D. Kumar, V. K. Jain, G. Shanker and A. Srivastava, *Process Biochem.*, 2003, **38**, 1731–1738, DOI: 10.1016/S0032-9592(02)00252-2.

27 M. C. A. Xavier, G. S. Dias, S. Hernalsteens and T. T. Franco, *ACS Omega*, 2025, **10**, 51891–51899, DOI: 10.1021/acsomega.5c08221.

28 X. Feng, B. Tang, Y. Jiang, Z. Xu, P. Lei, J. Liang and H. Xu, *J. Chem. Technol. Biotechnol.*, 2016, **91**, 2085–2093, DOI: 10.1002/jctb.4805.

29 S. G. Karp, A. L. Woiciechowski, V. T. Soccol and C. R. Soccol, *Braz. Arch. Biol. Technol.*, 2013, **56**, 679–689, DOI: 10.1590/S1516-89132013000400019.

30 T. A. Chimenez, M. H. Gehlen, K. Marabezi and A. A. S. Curvelo, *Cellulose*, 2014, **21**, 653–664, DOI: 10.1007/s10570-013-0135-9.

31 H. K. Gupta, P. Shivhare, T. K. Roy and N. J. Rao, *IPPTA*, 1997, **9**, 29–35.

32 J. M. Wolter, K. Schmeide, N. Huittinen and T. Stumpf, *Sci. Rep.*, 2019, **9**, 14255. DOI: 10.1038/s41598-019-50402-x

33 B. N. Brogdon and L. A. Lucia, *Tappi J.*, 2023, 22, 10, DOI: 10.32964/TJ22.10.631.

34 S. Sah, S. Maheshwari and A.Y. Kulkarni, *IPPTA*, 1982, **19**, 41–44.

35 X. Kang, A. Kirui, M. C. D. Widanage, F. Mentink-Vigier, D. J. Cosgrove and T. Wang, *Nat. Commun.*, 2019, **10**, 347, DOI: 10.1038/s41467-018-08252-0.

36 O. M. Terrett and P. Dupree, *Curr. Opin. Biotechnol.*, 2019, **56**, 97–104, DOI: 10.1016/j.copbio.2018.10.010.

37 S. Hellstén, J. Lahti, J. Heinonen, M. Kallioinen, M. Mänttäri and T. Sainio, *Chem. Eng. Res. Des.*, 2013, **91**, 2765–2774, DOI: 10.1016/j.cherd.2013.06.001.

38 T. Anttila, master thesis, Review of different kraft lignin separation technologies and comparing their effects on a kraft pulp mill, Aalto University, 2021. https://urn.fi/URN:NBN:fi:aalto-202109058984

View Article Online
DOI: 10.1039/D6GC01257D

Data availability statements

The authors declare that all the data that supports the findings of this study are available within the article and its ESI files or from the corresponding author upon reasonable request.